

Production of new superheavy Z=108-114 nuclei with ^{238}U , ^{244}Pu and $^{248,250}\text{Cm}$ targets

Zhao-Qing Feng,* Gen-Ming Jin, and Jun-Qing Li

Institute of Modern Physics, Chinese Academy of Sciences, Lanzhou 730000, People's Republic of China

(Dated: December 21, 2009)

Within the framework of the dinuclear system (DNS) model, production cross sections of new superheavy nuclei with charged numbers $Z=108-114$ are analyzed systematically. Possible combinations based on the actinide nuclides ^{238}U , ^{244}Pu and $^{248,250}\text{Cm}$ with the optimal excitation energies and evaporation channels are pointed out to synthesize new isotopes which lie between the nuclides produced in the cold fusion and the ^{48}Ca induced fusion reactions experimentally, which are feasible to be constructed experimentally. It is found that the production cross sections of superheavy nuclei decrease drastically with the charged numbers of compound nuclei. Larger mass asymmetries of the entrance channels enhance the cross sections in $2n-5n$ channels.

PACS number(s): 25.70.Jj, 24.10.-i, 25.60.Pj

The synthesis of superheavy nuclei (SHN) is motivated with respect to search the "island of stability" which is predicted theoretically, and has obtained much experimental research with fusion-evaporation reactions [1, 2]. Neutron-deficient SHN with charged numbers $Z=107-112$ were synthesized in cold fusion reactions with the ^{208}Pb and ^{209}Bi targets for the first time and investigated at GSI (Darmstadt, Germany) with the heavy-ion accelerator UNILAC and the SHIP separator [1, 3]. Recently, experiments on the synthesis of element 113 in the $^{70}\text{Zn}+^{209}\text{Bi}$ reaction have been performed successfully at RIKEN (Tokyo, Japan) [4]. More neutron-rich SHN with $Z=113-116$, 118 were assigned at FLNR in Dubna (Russia) with the double magic nucleus ^{48}Ca bombarding the actinide nuclei [2, 5, 6]. New heavy isotopes ^{259}Db and ^{265}Bh were also synthesized at HIRFL in Lanzhou (China) [7]. New SHN between the isotopes of the cold fusion and the ^{48}Ca induced reactions are of importance not only for investigating the structure of SHN such as influence of shell effect on stability of SHN etc, and also as a stepstone for further synthesizing and identifying heavier superheavy nuclei.

Here we use a dinuclear system (DNS) model [8, 9], in which the nucleon transfer is coupled to the relative motion by solving a set of microscopically derived master equations by distinguishing protons and neutrons, and a barrier distribution in the capture and fusion process of two colliding nuclei is introduced in the model. In the DNS model, the evaporation residue cross section is expressed as a sum over partial waves with angular

momentum J at centre-of-mass energy $E_{c.m.}$ [9, 10],

$$\sigma_{ER}(E_{c.m.}) = \frac{\pi\hbar^2}{2\mu E_{c.m.}} \sum_{J=0}^{J_{max}} (2J+1) T(E_{c.m.}, J) \times P_{CN}(E_{c.m.}, J) W_{sur}(E_{c.m.}, J). \quad (1)$$

Here, $T(E_{c.m.}, J)$ is the transmission probability of the two colliding nuclei overcoming the Coulomb barrier in the entrance channel to form the DNS. The P_{CN} is the probability that the system will evolve from a touching configuration to the formation of compound nucleus in competition with the quasi-fission of the DNS and the fission of heavy fragment. The last term is the survival probability of the formed compound nucleus, which can be estimated with the statistical evaporation model by considering the competition between neutron evaporation and fission [8].

Within the concept of the DNS, the fusion probability was also calculated by using the multidimensional Kramers-type expression to get the fusion and quasifission rate by Adamian *et al.* [11]. In order to describe the fusion dynamics as a diffusion process along proton and neutron degrees of freedom, the fusion probability is obtained by solving a set of master equations numerically in the potential energy surface of the DNS. The time evolution of the distribution probability function $P(Z_1, N_1, E_1, t)$ for fragment 1 with proton number Z_1 and neutron number N_1 and with excitation energy E_1 is described by the following master equations,

$$\frac{dP(Z_1, N_1, E_1, t)}{dt} = \sum_{Z'_1} W_{Z_1, N_1; Z'_1, N_1}(t) [d_{Z_1, N_1} P(Z'_1, N_1, E'_1, t) - d_{Z'_1, N_1} P(Z_1, N_1, E_1, t)] + \sum_{N'_1} W_{Z_1, N_1; Z_1, N'_1}(t) [d_{Z_1, N_1} P(Z_1, N'_1, E'_1, t) - d_{Z_1, N'_1} P(Z_1, N_1, E_1, t)] - [\Lambda_{qf}(\Theta(t)) + \Lambda_{fis}(\Theta(t))] P(Z_1, N_1, E_1, t) \quad (2)$$

Here $W_{Z_1, N_1; Z'_1, N_1}$ ($W_{Z_1, N_1; Z_1, N'_1}$) is the mean transition

probability from the channel (Z_1, N_1, E_1) to (Z'_1, N_1, E'_1)

(or (Z_1, N_1, E_1) to (Z_1, N'_1, E'_1)), and d_{Z_1, N_1} denotes the microscopic dimension corresponding to the macroscopic state (Z_1, N_1, E_1) . The sum is taken over all possible proton and neutron numbers that fragment Z'_1, N'_1 may take, but only one nucleon transfer is considered in the model with the relation $Z'_1 = Z_1 \pm 1$ and $N'_1 = N_1 \pm 1$. The excitation energy E_1 is determined by the dissipation energy from the relative motion and the potential energy surface of the DNS. The motion of nucleons in the interacting potential is governed by the single-particle Hamiltonian [8, 9]. The evolution of the DNS along the variable R leads to the quasi-fission of the DNS. The quasi-fission rate Λ_{qf} and the fission rate Λ_{fis} of heavy fragment are estimated with the one-dimensional Kramers formula [9, 10].

In the relaxation process of the relative motion, the DNS will be excited by the dissipation of the relative kinetic energy. The local excitation energy is determined by the excitation energy of the composite system and the potential energy surface of the DNS. The potential energy surface (PES) of the DNS is given by

$$U(\{\alpha\}) = B(Z_1, N_1) + B(Z_2, N_2) - [B(Z, N) + V_{rot}^{CN}(J)] + V(\{\alpha\}) \quad (3)$$

with $Z_1 + Z_2 = Z$ and $N_1 + N_2 = N$. Here the symbol $\{\alpha\}$ denotes the sign of the quantities $Z_1, N_1, Z_2, N_2; J, \mathbf{R}; \beta_1, \beta_2, \theta_1, \theta_2$. The $B(Z_i, N_i)$ ($i = 1, 2$) and $B(Z, N)$ are the negative binding energies of the fragment (Z_i, N_i) and the compound nucleus (Z, N) , respectively, which are calculated from the liquid drop model, in which the shell and the pairing corrections are included reasonably. The V_{rot}^{CN} is the rotation energy of the compound nucleus. The β_i represent the quadrupole deformations of the two fragments. The θ_i denote the angles between the collision orientations and the symmetry axes of deformed nuclei. The interaction potential between fragment (Z_1, N_1) and (Z_2, N_2) includes the nuclear, Coulomb and centrifugal parts, the details are given in Ref. [9]. In the calculation, the distance \mathbf{R} between the centers of the two fragments is chosen to be the value which gives the minimum of the interaction potential, in which the DNS is considered to be formed. So the PES depends on the proton and neutron numbers of the fragments.

The formation probability of the compound nucleus at the Coulomb barrier B and for the angular momentum J is given by [8, 9]

$$P_{CN}(E_{c.m.}, J, B) = \sum_{Z_1=1}^{Z_{BG}} \sum_{N_1=1}^{N_{BG}} P(Z_1, N_1, E_1, \tau_{int}). \quad (4)$$

The interaction time τ_{int} in the dissipation process of two colliding partners is dependent on the incident energy $E_{c.m.}$ and the quantities J and B . We obtain the fusion

probability as

$$P_{CN}(E_{c.m.}, J) = \int f(B) P_{CN}(E_{c.m.}, J, B) dB, \quad (5)$$

where the barrier distribution function is taken as an asymmetric Gaussian form.

Neutron-deficient SHN with charged numbers $Z=107-113$ were synthesized successfully in the cold fusion reactions. The evaporation residues was observed by the consecutive α decay until to take place the spontaneous fission of the known nuclides, in which the fusion dynamics and the structure properties of the compound nucleus have a strong influence in the production of SHN. Recently more neutron-rich and heavier SHN with charged numbers $Z=113-116, 118$ were produced in the fusion-evaporation reactions of ^{48}Ca bombarding actinide targets. Superheavy residues were also identified by the consecutive α decay, unfortunately to spontaneous fission of unknown nuclides. Neutron-rich projectile-target combinations are necessary to be chosen so that superheavy residues approach the "island of stability" with the doubly magic shell closure beyond ^{208}Pb at the position of protons $Z=114-126$ and neutrons $N=184$. New SHN between the isotopes of the cold fusion and the ^{48}Ca induced reactions are of importance for the structure studies themselves and also as daughter nuclides for identifying heavier SHN in the future.

The excitation energy of compound nucleus is obtained by $E_{CN}^* = E_{c.m.} + Q$, where $E_{c.m.}$ is the incident energy in the center-of-mass system. The Q value is given by $Q = \Delta M_P + \Delta M_T - \Delta M_C$, and the corresponding mass defects are taken from Ref. [12] for projectile, target and compound nucleus, respectively. Usually, neutron-rich projectiles are used to synthesize SHN experimentally, such as ^{64}Ni and ^{70}Zn in the cold fusion reactions, which can enhance the survival probability W_{sur} in Eq.(1) of the excited compound nucleus owing to smaller neutron separation energy. Within the framework of the DNS model, we calculated the evaporation residue cross sections of superheavy element Mt based on the actinide targets $^{248,250}\text{Cm}$, ^{244}Pu and ^{238}U with the neutron-rich projectiles ^{27}Al , ^{31}P and ^{37}Cl as shown in Fig. 1. One can see that the 3n channel in the reactions $^{27}\text{Al}+^{248}\text{Cm}$ and $^{37}\text{Cl}+^{238}\text{U}$, and the 4n and 5n channels in the system $^{27}\text{Al}+^{250}\text{Cm}$ have the larger cross sections in the production of SHN ^{272}Mt and ^{273}Mt . Superheavy element Ds($Z=110$) was successfully synthesized in the cold fusion reactions [1, 13]. The production of the SHN depends on the isotopic combinations of projectiles and targets. Calculations were performed for the reactions $^{30}\text{Si}+^{248,250}\text{Cm}$, $^{36}\text{S}+^{244}\text{Pu}$ and $^{40}\text{Ar}+^{238}\text{U}$ to produce superheavy element Ds as shown in Fig. 2. Combination with ^{248}Cm has the larger cross section in the 4n channel than the isotope ^{250}Cm due to the larger value of survival probability. The 4n channels in the systems $^{30}\text{Si}+^{248,250}\text{Cm}$ and $^{40}\text{Ar}+^{238}\text{U}$ and the 3n channel in

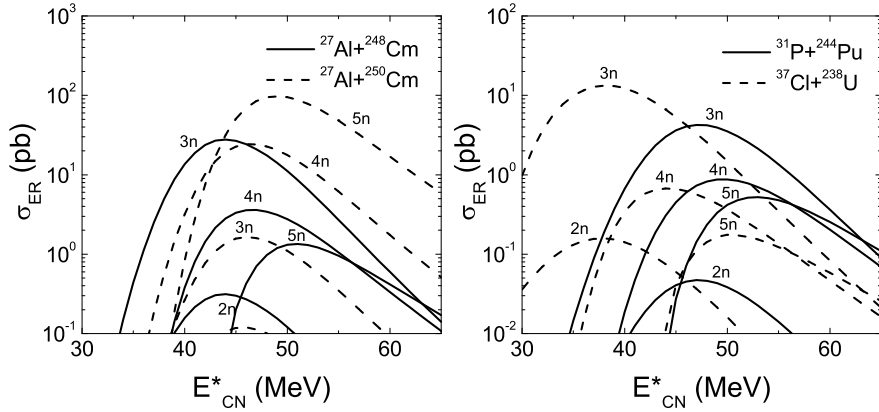


FIG. 1. Evaporation residue excitation functions in the production of isotopes of superheavy element Mt in the reactions $^{27}\text{Al}+^{248,250}\text{Cm}$, $^{31}\text{P}+^{244}\text{Pu}$ and $^{37}\text{Cl}+^{238}\text{U}$.

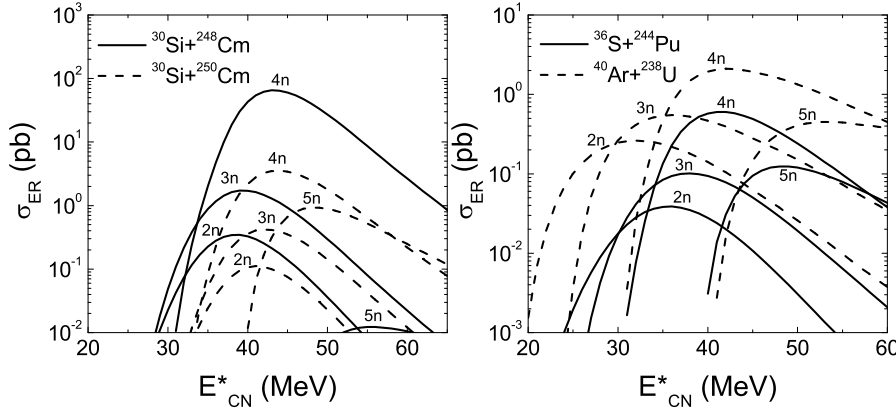


FIG. 2. Calculated production cross sections for the reactions $^{30}\text{Si}+^{248,250}\text{Cm}$, $^{36}\text{S}+^{244}\text{Pu}$ and $^{40}\text{Ar}+^{238}\text{U}$ to produce superheavy element Ds.

the reaction $^{30}\text{Si}+^{248}\text{Cm}$ are feasible in the synthesis of new SHN $^{274-276}\text{Ds}$. These combinations can be chosen in experimental preparation with the present facilities.

In the DNS model, the isotopic trends are mainly determined by both the fusion and survival probabilities. When the neutron number of the projectile is increasing, the DNS gets more symmetrical and the fusion probability decreases if the DNS does not consist of more stable nuclei due to a higher inner fusion barrier. A smaller neutron separation energy and a larger shell correction lead to a larger survival probability. The compound nucleus with closed neutron shells has larger shell correction energy and neutron separation energy. The cross section decreases rapidly in the production of the isotopes of Rg(Z=111). Optical channels are the 4n evaporation for

the systems $^{31}\text{P}+^{248,250}\text{Cm}$, $^{37}\text{Cl}+^{244}\text{Pu}$ and $^{41}\text{K}+^{238}\text{U}$ to produce $^{275,277}\text{Rg}$ as shown in Fig. 3. Superheavy element Z=112 is more difficult to be produced in the selected systems. Shown in Fig. 5 gives that the possible way is the 4n channel in the reaction $^{36}\text{S}+^{250}\text{Cm}$, but the cross section is still smaller than the system $^{48}\text{Ca}+^{238}\text{U}$ [10] although the larger mass asymmetry.

The productions of superheavy element Z=113 were successfully performed in the cold fusion reaction $^{70}\text{Zn}+^{209}\text{Bi}$ [4] and also in the hot fusion $^{48}\text{Ca}+^{237}\text{Np}$ [14] with the cross section less than 1 pb. We calculated the evaporation residue excitation functions for the reactions $^{37}\text{Cl}+^{248,250}\text{Cm}$, $^{41}\text{K}+^{244}\text{Pu}$ and $^{45}\text{Sc}+^{238}\text{U}$. The results show that the 3n and 4n channels in the systems $^{37}\text{Cl}+^{248,250}\text{Cm}$ have larger cross sections and are

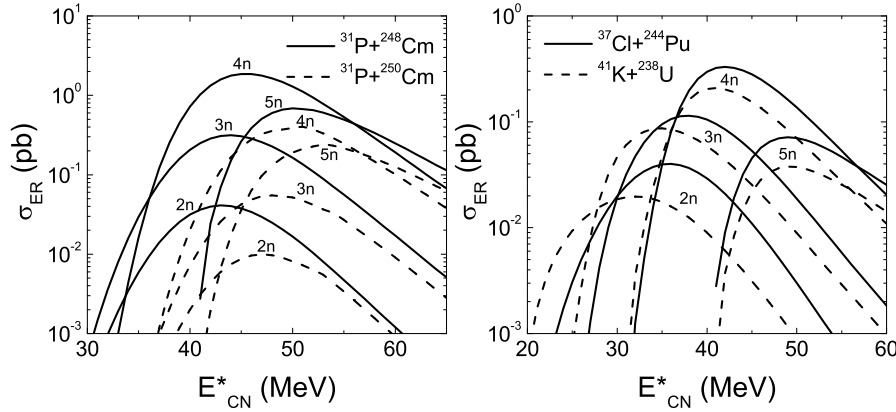


FIG. 3. The same as in Fig. 1, but for the reactions $^{31}\text{P} + ^{248,250}\text{Cm}$, $^{37}\text{Cl} + ^{244}\text{Pu}$ and $^{41}\text{K} + ^{238}\text{U}$ to produce superheavy element Rg.

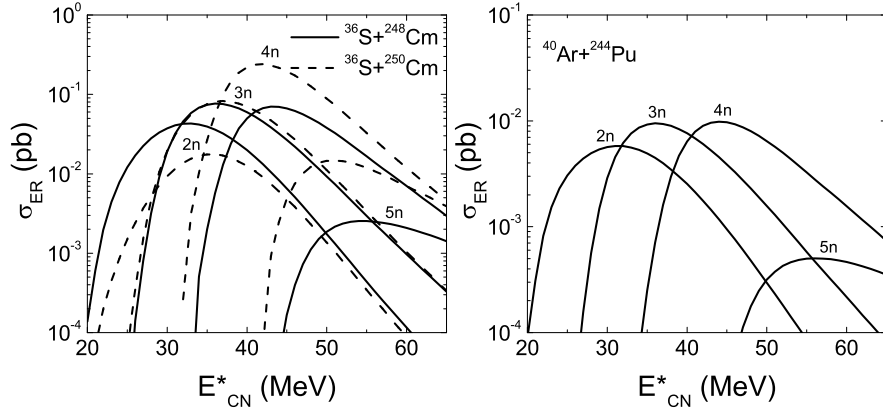


FIG. 4. Comparison of the calculated production cross sections in the reactions $^{36}\text{S} + ^{248,250}\text{Cm}$ and $^{40}\text{Ar} + ^{244}\text{Pu}$ to synthesize superheavy element Z=112.

possible to synthesize new isotopes $^{281-284}\text{Rg}$ in experimentally. Superheavy element Z=114 is difficult to be produced from our calculations for the selected systems because of the smaller cross sections with less than 0.1 pb for all systems. We list the maximal production cross sections and the corresponding excitation energies in the brackets calculated by using the DNS model in Table 1. These selected systems and evaporation channels are feasible to produce new isotopes between the cold fusion and the ^{48}Ca induced fusion reactions.

In summary, we systematically investigated the production of superheavy residues in the fusion-evaporation reactions using the DNS model, in which the nucleon transfer leading to the formation of superheavy compound nucleus is described by a set of microscopically

derived master equations distinguishing the proton and neutron transfer that are coupled to the dissipation of relative motion energy and angular momentum. The production of new isotopes between the gap of the cold fusion and the ^{48}Ca induced fusion reactions are discussed for selected systems. Optimal evaporation channels and excitation energies corresponding to the maximal cross sections are stated and discussed systematically.

We would like to thank Prof. Werner Scheid for carefully reading the manuscript. This work was supported by the National Natural Science Foundation of China under Grant Nos. 10805061 and 10775061, the special foundation of the president fund, the west doctoral project of Chinese Academy of Sciences, and major state basic research development program under Grant No.

TABLE I. Comparisons of calculated maximal evaporation residue cross sections and optimal excitation energies (in bracket) in 2n-5n channels.

Reactions	σ_{ER}^{2n} (pb) (E_{CN}^*)	σ_{ER}^{3n} (pb) (E_{CN}^*)	σ_{ER}^{4n} (pb) (E_{CN}^*)	σ_{ER}^{5n} (pb) (E_{CN}^*)
$^{26}\text{Mg} + ^{248}\text{Cm}$	2.50 (40 MeV)	26.2 (40 MeV)	719.1 (42 MeV)	1.23 (51 MeV)
$^{26}\text{Mg} + ^{250}\text{Cm}$	1.11 (41 MeV)	10.57 (41 MeV)	185.2 (42 MeV)	108.5 (45 MeV)
$^{30}\text{Si} + ^{244}\text{Pu}$	0.46 (42 MeV)	5.09 (43 MeV)	185.1 (44 MeV)	0.72 (51 MeV)
$^{36}\text{S} + ^{238}\text{U}$	0.21 (37 MeV)	1.96 (38 MeV)	42.97 (42 MeV)	0.11 (52 MeV)
$^{27}\text{Al} + ^{248}\text{Cm}$	0.31 (44 MeV)	27.83 (44 MeV)	3.59 (47 MeV)	1.34 (51 MeV)
$^{27}\text{Al} + ^{250}\text{Cm}$	0.12 (46 MeV)	1.64 (46 MeV)	24.31 (46 MeV)	97.44 (49 MeV)
$^{31}\text{P} + ^{244}\text{Pu}$	4.71×10^{-2} (47 MeV)	4.25 (47 MeV)	0.87 (50 MeV)	0.52 (53 MeV)
$^{37}\text{Cl} + ^{238}\text{U}$	0.16 (38 MeV)	13.31 (38 MeV)	0.67 (44 MeV)	0.17 (50 MeV)
$^{30}\text{Si} + ^{248}\text{Cm}$	0.34 (39 MeV)	1.72 (39 MeV)	65.32 (43 MeV)	1.22×10^{-2} (56 MeV)
$^{30}\text{Si} + ^{250}\text{Cm}$	0.11 (41 MeV)	0.42 (42 MeV)	3.54 (44 MeV)	0.93 (48 MeV)
$^{36}\text{S} + ^{244}\text{Pu}$	3.87×10^{-2} (36 MeV)	0.101 (38 MeV)	0.61 (41 MeV)	0.12 (48 MeV)
$^{40}\text{Ar} + ^{238}\text{U}$	0.26 (32 MeV)	0.55 (36 MeV)	2.10 (42 MeV)	0.45 (53 MeV)
$^{31}\text{P} + ^{248}\text{Cm}$	4.11×10^{-2} (43 MeV)	0.31 (44 MeV)	1.85 (45 MeV)	0.69 (50 MeV)
$^{31}\text{P} + ^{250}\text{Cm}$	9.91×10^{-3} (47 MeV)	5.49×10^{-2} (48 MeV)	0.41 (51 MeV)	0.25 (52 MeV)
$^{37}\text{Cl} + ^{244}\text{Pu}$	4.01×10^{-2} (36 MeV)	0.11 (38 MeV)	0.33 (42 MeV)	7.15×10^{-2} (49 MeV)
$^{41}\text{K} + ^{238}\text{U}$	1.96×10^{-2} (32 MeV)	8.67×10^{-2} (35 MeV)	0.21 (41 MeV)	3.77×10^{-2} (49 MeV)
$^{36}\text{S} + ^{248}\text{Cm}$	4.31×10^{-2} (33 MeV)	7.64×10^{-2} (36 MeV)	7.02×10^{-2} (43 MeV)	2.55×10^{-3} (54 MeV)
$^{36}\text{S} + ^{250}\text{Cm}$	1.76×10^{-2} (36 MeV)	8.25×10^{-2} (37 MeV)	0.24 (42 MeV)	1.47×10^{-2} (51 MeV)
$^{40}\text{Ar} + ^{244}\text{Pu}$	5.79×10^{-3} (31 MeV)	9.48×10^{-3} (36 MeV)	9.84×10^{-3} (44 MeV)	5.02×10^{-4} (56 MeV)
$^{37}\text{Cl} + ^{248}\text{Cm}$	5.81×10^{-2} (31 MeV)	0.26 (35 MeV)	0.195 (42 MeV)	1.05×10^{-2} (52 MeV)
$^{37}\text{Cl} + ^{250}\text{Cm}$	2.08×10^{-2} (35 MeV)	0.21 (36 MeV)	0.594 (41 MeV)	7.06×10^{-2} (49 MeV)
$^{41}\text{K} + ^{244}\text{Pu}$	1.11×10^{-2} (29 MeV)	4.22×10^{-2} (34 MeV)	3.31×10^{-2} (42 MeV)	2.3×10^{-3} (53 MeV)
$^{45}\text{Sc} + ^{238}\text{U}$	1.72×10^{-2} (27 MeV)	1.99×10^{-2} (35 MeV)	2.32×10^{-3} (45 MeV)	1.92×10^{-4} (57 MeV)
$^{40}\text{Ar} + ^{248}\text{Cm}$	6.98×10^{-3} (26 MeV)	2.21×10^{-2} (33 MeV)	3.5×10^{-2} (41 MeV)	2.12×10^{-3} (51 MeV)
$^{40}\text{Ar} + ^{250}\text{Cm}$	2.77×10^{-3} (29 MeV)	2.11×10^{-2} (33 MeV)	7.96×10^{-2} (40 MeV)	9.69×10^{-3} (48 MeV)
$^{48}\text{Ti} + ^{238}\text{U}$	4.51×10^{-2} (24 MeV)	1.37×10^{-2} (32 MeV)	5.81×10^{-3} (42 MeV)	1.71×10^{-4} (54 MeV)
$^{50}\text{Ti} + ^{238}\text{U}$	5.11×10^{-2} (23 MeV)	2.18×10^{-2} (31 MeV)	1.07×10^{-2} (40 MeV)	4.11×10^{-4} (50 MeV)

2007CB815000.

* fengzhq@impcas.ac.cn

[1] S. Hofmann and G. Münzenberg, Rev. Mod. Phys. **72**, 733 (2000); S. Hofmann, Rep. Prog. Phys. **61**, 639 (1998).

[2] Yu. Ts. Oganessian, J. Phys. G **34**, R165 (2007).

[3] G. Münzenberg, J. Phys. G **25**, 717 (1999).

[4] K. Morita, K. Morimoto, D. Kaji *et al.*, J. Phys. Soc. Jpn. **73**, 2593 (2004).

[5] Yu. Ts. Oganessian, V. K. Utyonkov, Yu. V. Lobanov *et al.*, Phys. Rev. C **69**, 021601(R) (2004).

[6] Yu. Ts. Oganessian, V. K. Utyonkov, Yu. V. Lobanov *et al.*, Phys. Rev. C **74**, 044602 (2006).

[7] Z. G. Gan, Z. Qin, H. M. Fan *et al.*, Eur. Phys. J. **A10**, 21 (2001); Z. G. Gan, J. S. Guo, X. L. Wu *et al.*, Eur. Phys. J. **A20**, 385 (2004).

[8] Z. Q. Feng, G. M. Jin, F. Fu and J. Q. Li, Nucl. Phys. **A771**, 50 (2006).

[9] Z. Q. Feng, G. M. Jin, J. Q. Li and W. Scheid, Phys. Rev. C **76**, 044606 (2007).

[10] Z. Q. Feng, G. M. Jin, J. Q. Li and W. Scheid, Nucl. Phys. **A816**, 33 (2009).

[11] G. G. Adamian, N. V. Antonenko, W. Scheid *et al.*, Nucl. Phys. **A627**, 361 (1997); Nucl. Phys. **A633**, 409 (1998).

[12] P. Möller *et al.*, At. Data Nucl. Data Tables **59**, 185 (1995).

[13] S. Hofmann, V. Ninov, F.P. Heßberger *et al.*, Z. Phys. A **350**, 277 (1995); Z. Phys. A **350**, 281 (1995).

[14] Yu. Ts. Oganessian, V. K. Utyonkov, Yu. V. Lobanov *et al.*, Phys. Rev. C **76**, 011601(R) (2007).